

Perovskites



Development of Double-Perovskite Compounds as Cathode Materials for Low-Temperature Solid Oxide Fuel Cells**

Seonyoung Yoo, Areum Jun, Young-Wan Ju, Dorj Odkhuu, Junji Hyodo, Hu Young Jeong, Noejung Park, Jeeyoung Shin, Tatsumi Ishihara, and Guntae Kim*

Abstract: A class of double-perovskite compounds display fast oxygen ion diffusion and high catalytic activity toward oxygen reduction while maintaining excellent compatibility with the electrolyte. The astoundingly extended stability of $\text{NdBa}_{1-x}\text{Ca}_x\text{Co}_2\text{O}_{5+\delta}$ (NBCaCO) under both air and CO_2 -containing atmosphere is reported along with excellent electrochemical performance by only Ca doping into the A site of $\text{NdBaCo}_2\text{O}_{5+\delta}$ (NBCO). The enhanced stability can be ascribed to both the increased electron affinity of mobile oxygen species with Ca, determined through density functional theory calculations and the increased redox stability from the coulometric titration.

Solid oxide fuel cells (SOFCs) are promising fuel cells that offer very high efficiency and long-term stability. To make SOFC technology affordable, however, the operating temperature must be reduced so that much less expensive materials can be used for other cell components during cell fabrication and/or operation.^[1–7] To overcome these problems, researchers have strived to lower the operating temperature of SOFCs toward a low-temperature (LT) range (500–650 °C). One of the challenges for LT-SOFCs, however, is to develop cathode materials with sufficiently high electrocatalytic activity for oxygen reduction. Intensive research has thus been carried out to explore alternative cathode materials that achieve superior and stable electrochemical performance.^[8–12]

Recently, many groups have focused on $\text{LnBaMO}_{5+\delta}$ (Ln = Pr, Nd, Sm, and Gd, M = Co, Fe, Ni, Cu, etc.) layered perovskite oxides, based on their much higher chemical diffusion and surface-exchange coefficients compared to those of ABO_3 -type perovskite oxides. In particular, cobalt-containing layered oxides, $\text{PrBaCo}_2\text{O}_{5+\delta}$ (PBCO),^[13] offer

faster oxygen ion diffusion and surface-exchange kinetics, leading to very low area-specific resistance (ASR) and good cell performance.^[14]

Our group has extensively studied a class of double-perovskite oxides,^[15–18] $\text{NdBaCo}_2\text{O}_{5+\delta}$ (NBCO), with the aim of exploiting their high electrical conductivity and high catalytic activity for the oxygen reduction reaction (ORR). We have found that Sr doping into the Ba site enhanced the electrical conductivity and the ORR. However, some drawbacks such as redox instability and formation of secondary phase, e.g., BaCO_3 or SrCO_3 , arise from the reaction with CO_2 in the atmosphere.^[19,20] In this regard, Lee et al.^[21] demonstrated dopant segregation occurring from the A site of a perovskite with different dopants, such as Ba, Sr, and Ca. They reported that a smaller size mismatch between the host and dopant cations reduced the segregation level of the dopant, leading to more stable cathode surfaces. Hence, Ca doping at the A site of NBCO is anticipated to suppress surface segregation, resulting in better long-term stability of the cathode. There is thus a strong motivation to utilize the favorable properties of Co-rich materials and simultaneously the higher chemical stability originating from the dopants.^[22]

Herein, we present excellent electrochemical performance and stability under operating conditions by only Ca doping into the A site of the double-perovskite structure as a potential cathode material. In addition, we studied the effects of Ca doping on electrical properties, oxygen kinetics, redox properties, and morphology for application of NBCaCO as a superior cathode material for LT-SOFCs.

The ideal double-perovskite structure of $\text{NdBaCo}_2\text{O}_{5+\delta}$ compounds can be generated by the stacking sequence ...BaO/CoO₂/NdO_x/CoO₂..., which is closely related to the

[*] S. Yoo, A. Jun, Prof. G. Kim
Department of Energy Engineering, UNIST
Ulsan, 689-798 (Korea)
E-mail: gtkim@unist.ac.kr
Dr. D. Odkhuu, Prof. N. Park
Department of Physics, School of Natural Science
Center for Multidimensional Carbon Materials, UNIST
Ulsan, 689-798 (Korea)
Dr. Y.-W. Ju, Dr. J. Hyodo, Prof. T. Ishihara
Department of Applied Chemistry, Faculty of Engineering, Kyushu University
Fukuoka, 819-0395 (Japan)
Prof. T. Ishihara
International Institute for Carbon Neutral Energy Research, Kyushu University
Fukuoka 819-0395 (Japan)

Prof. H. Y. Jeong
UNIST Central Research Facilities (UCRF), UNIST
Ulsan, 689-798 (Korea)
Prof. J. Shin
Department of Mechanical Engineering, Dong-Eui University
Busan 614-714 (Korea)

[**] This research was supported by the Mid-career Researcher Program (2013R1A2A2A04015706) funded by the Korea Government Ministry of Science, ICT and Future Planning and the Basic Science Research Program (2010-0021214) funded by the Ministry of Education through the National Research Foundation of Korea. It was also supported by the New & Renewable Energy of the Korea Institute of Energy Technology Evaluation and Planning (KETEP; 20113020030060) grant funded by the Korea Ministry of Knowledge Economy.



Supporting information for this article is available on the WWW under <http://dx.doi.org/10.1002/anie.201407006>.

cuprate superconductors depicted in Figure 1a. Mobile oxygen species are located between the NdO layers and may show highly anisotropic oxygen diffusion depending on directions.^[13] To directly observe atom arrangements of ordered NBCaCO, we used high-angle annular dark-field (HAADF) scanning transmission electron microscopy (STEM) with a probe-side aberration corrector. Because

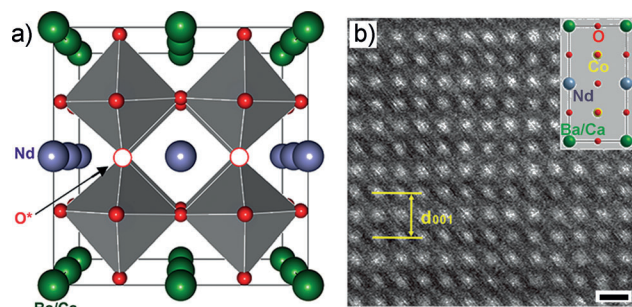


Figure 1. a) Crystal structure of $\text{NdBa}_{0.75}\text{Ca}_{0.25}\text{Co}_2\text{O}_{5+\delta}$ (NBCaCO). b) HAADF STEM image of an NBCaCO sample. Scale bar = 0.5 nm.

the contrast in STEM images increases with the atomic number of elements, brighter atoms can be matched with a heavy element (Nd) and darker atoms can be assigned as Ba/Ca atoms, as shown in Figure 1b.

The development of new cathode materials with high electrocatalytic activity for the ORR is of great importance for operation at low temperature. As shown in Figure 2a and b, the ASR values of NBCaCO are dramatically reduced to $0.066 \Omega\text{cm}^2$ at 600°C compared to that of NBCO ($0.091 \Omega\text{cm}^2$). Based on previous reports,^[23] the large pop-

ulation of mobile oxygen species may contribute to enhanced oxygen kinetics associated with oxygen bulk diffusion and surface exchange. Therefore, a higher concentration of mobile oxygen species in the Ln–O layer as a result of Ca doping may lead to faster oxygen kinetics and better electrochemical performance.

Identification of the surface exchange and oxygen bulk diffusion properties will be helpful in understanding the electrochemical properties required for cathode function. The average oxygen tracer diffusion coefficients are represented in an Arrhenius plot in Figure 2c for the entire temperature range and compared with the published data.

The measured diffusion coefficients are quite high, ranging from 9.9×10^{-10} to $4.37 \times 10^{-8} \text{ cm}^2 \text{ s}^{-1}$ at a temperature range from 413 to 648°C . These D^* values are clearly higher than those of $\text{PrBaCo}_2\text{O}_{5+\delta}$ (PBCO) and $\text{GdBaCo}_2\text{O}_{5+\delta}$ (GBCO) with similar structures.^[24,25] In addition, it can be confirmed that Ca doping imposes a favorable effect on not only electrical conductivity but also diffusivity. On the other hands, in the case of the surface-exchange coefficients (Figure 2d), the effect of Ca doping does not appear to be substantial. Even though Ca doping results in a change in surface-exchange coefficients between NBCO and NBCaCO, both exhibit much higher surface-exchange coefficients than other materials (PBCO and GBCO). It is thus confirmed that the lower ASR with Ca doping in the NBCO can be partly explained by the high oxygen surface exchange and gas-phase diffusion characteristics of NBCaCO.

To assess the performance and durability of new NBCaCO cathode materials, the typical single cell performance of the NBCaCO cathodes is measured using a Ni-GDC anode-supported cell based on a approximately $15 \mu\text{m}$ thick GDC electrolyte. Figure 3a shows typical I - V curves and the corresponding power densities of single cells with NBCO-GDCs and NBCaCO-GDCs as the cathodes at 600°C . The maximum power densities of the NBCO-GDCs and NBCaCO-GDCs single cells were 1.647 W cm^{-2} and 2.114 W cm^{-2} , respectively, at 600°C . The single-cell performances are enhanced with Ca doping in NBCO, which can be anticipated from the behavior of the total conductivities and area-specific resistance (ASR) with Ca doping.

Stability of SOFC materials is also a key impediment for the commercial success of various low-temperature SOFCs, although high power density is still necessary. Regarding the stability of a $\text{NdBa}_{1-x}\text{Ca}_x\text{Co}_2\text{O}_{5+\delta} | \text{GDC} | \text{Ni-GDC}$ single cell, as shown in Figure 3c, the voltage of NBCaCO-GDCs and NBCO-GDCs single cells was recorded as a function of time under a constant current load of 0.6 V , operating in humidified H_2 as the fuel and stationary air as the oxidant at 550°C . After operation for 150 h , the current density of the NBCO single cell decreased dramatically by about 50% , while that of the NBCaCO-GDCs single cell remained almost constant with no degradation. The NBCaCO-GDCs single cell exhibited excellent stability, demonstrating the high potential of NBCaCO as an LT-SOFC cathode material.

In order to predict the stability of mobile oxygen species (O^*) in NBCaCO, we performed first-principles

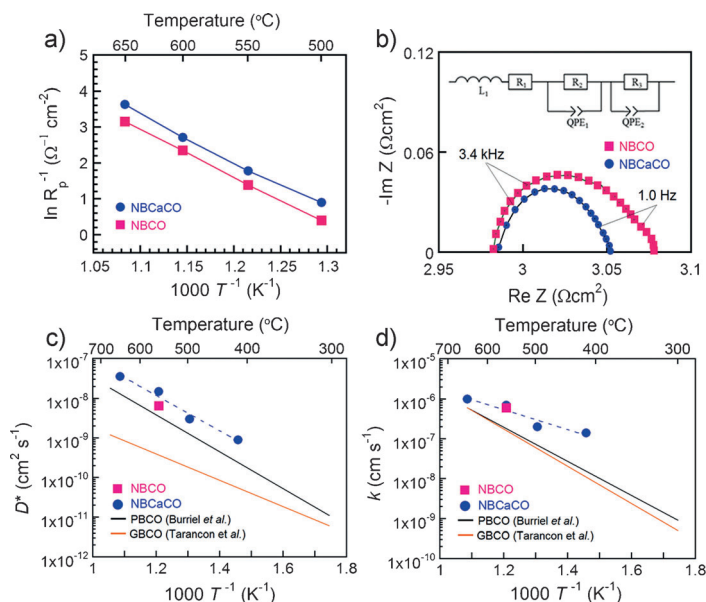


Figure 2. a) Arrhenius plot of reciprocal ASR. Activation energy for $x=0$: $109.568 \pm 1.39 \text{ kJ mol}^{-1}$, for $x=0.25$: $108.153 \pm 4.71 \text{ kJ mol}^{-1}$. b) ASR under open-circuit conditions at 600°C . c) Arrhenius plots of oxygen tracer diffusivity (D^*). d) Arrhenius plots of surface-oxygen-exchange coefficient (k).

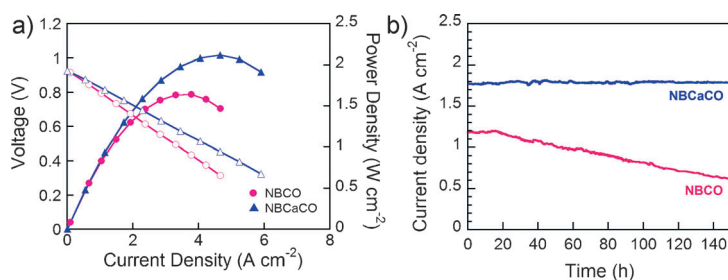


Figure 3. Electrochemical performances and long-term stability data. a) *I*-*V* curves and the corresponding power densities of test cells at 600 °C. b) Long-term stability measurement at a constant cell voltage of 0.6 V at 550 °C.

density functional theory (DFT) calculations for the formation energy of O*, defined as

$$E_f = E_{\text{tot}}(\delta = 1) - E_{\text{tot}}(\delta = 0) - N\mu_{\text{O}} \quad (1)$$

where $E_{\text{tot}}(\delta=1)$ and $E_{\text{tot}}(\delta=0)$ are the total energies of systems with and without O*, respectively. N is the number of O* atoms in the unit cell, μ_{O} is the chemical potential of an O atom, which is taken as the total energy of an O atom in an isolated O₂ molecule. The calculated formation energy of O* in NBCaCO is shown in Figure 4a, and compared to those in

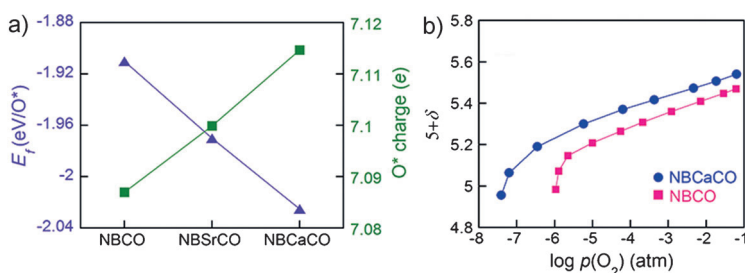


Figure 4. a) The formation energy (left) and Bader charge (right) of O* (mobile oxygen species). b) Oxygen nonstoichiometry as a function of $p(\text{O}_2)$ at 700 °C.

NBCO and Sr-doped NBSrCO. The formation energies are negative for these three systems, and the magnitude increases monotonically from NBCO to NBSrCO to NBCaCO. This result indicates that Ca doping for the Ba site leads to excellent stability for O* atoms in NBCO.

With regard to stability, cathode materials with high redox and thermal stability should be developed for low-temperature operation. Under operating conditions, the interface of SOFCs between the electrolyte and the cathode experiences a low $p(\text{O}_2)$, which may cause redox degradation of the cathode and affect the long-term stability of the cathode performance.^[19] If a new electrode material possesses poor redox properties or is decomposed at the fuel cell operating temperature and $p(\text{O}_2)$ range, it cannot be used as an electrode. Sufficient electrical conductivity at relatively low $p(\text{O}_2)$ is also important to ensure efficient current collection and long-term stability of the cell.

To confirm the redox properties and electrical conductivities at low $p(\text{O}_2)$, oxygen nonstoichiometry of the NBCaCO

and NBCO samples was investigated as a function of $p(\text{O}_2)$ at 700 °C (Figure S4c) by coulometric titration. The isotherm of NBCaCO shows a lower $p(\text{O}_2)$ for decomposition than that of NBCO, implying that NBCaCO has a higher redox stability and sufficient electrical conductivity under cathodic polarization. Its redox properties related to oxygen thermodynamics, such as the oxidation enthalpies and entropies of NBCaCO, were investigated using the results (Figure S11). The detailed proofs of related equations have been described elsewhere.^[15,26] There are dramatic changes in the oxidation enthalpies according to the extent of reduction.

The values of $-\Delta H$ become lower for a higher oxygen content (δ), implying that lower energy is needed for the evolution of the mobile oxygen species (Figure S11). Therefore, through the thermodynamic behavior, it is also confirmed that NBCaCO is more stable than NBCO, considering its higher oxidation enthalpy near the cathode-operating conditions. These results indicate that Ca doping provides favorable properties for practical applications in LT-SOFCs, that is, higher redox stability of the NBCaCO oxides, which can be a key factor for achieving stable electrochemical properties of a cathode material for viable operation of LT-SOFCs.^[27]

A class of cation-ordered, double-perovskite compounds display fast oxygen ion diffusion and high catalytic activity toward the ORR at low temperatures, while maintaining excellent compatibility with the electrolyte under typical fuel-cell operating conditions. The structural characteristics, electrical properties, electrochemical performances, and redox and performance stability of NBCaCO are investigated with respect to the effects of Ca doping on the Ba site in NBCO and a DFT analysis is carried out to evaluate its cathode material for LT-SOFC applications. The maximum power density of the NBCaCO single cell was 2.114 W cm⁻² at 600 °C and the typical cell performance of NBCaCO was very stable at 550 °C for 150 h as compared with that of NBCO. A more comprehensive understanding of the mechanistic details may help to envision the design of improved double-perovskite cathode materials for a new generation of high-performance SOFCs with enhanced durability.

Received: July 15, 2014

Published online: September 8, 2014

Keywords: ceramics · electrochemistry · energy conversion · fuel cells · perovskite phases

- [1] Z. L. Zhan, S. A. Barnett, *Science* **2005**, 308, 844–847.
- [2] Y. Choi, M. C. Lin, M. Liu, *Angew. Chem. Int. Ed.* **2007**, 46, 7214–7219; *Angew. Chem.* **2007**, 119, 7352–7357.
- [3] S. D. Park, J. M. Vohs, R. J. Gorte, *Nature* **2000**, 404, 265–267.
- [4] E. D. Wachsman, K. T. Lee, *Science* **2011**, 334, 935–939.
- [5] L. Yang, S. Z. Wang, K. Blinn, M. F. Liu, Z. Liu, Z. Cheng, M. Liu, *Science* **2009**, 326, 126–129.

- [6] Y. H. Huang, R. I. Dass, Z. L. Xing, J. B. Goodenough, *Science* **2006**, 312, 254–257.
- [7] M. Mogensen, K. V. Jensen, M. J. Jorgensen, S. Primdahl, *Solid State Ionics* **2002**, 150, 123–129.
- [8] W. Zhou, J. Sunarso, M. Zhao, F. Liang, T. Klande, A. Feldhoff, *Angew. Chem. Int. Ed.* **2013**, 52, 14036–14040; *Angew. Chem.* **2013**, 125, 14286–14290.
- [9] Z. Shao, C. Zhong, W. Wang, C. Su, W. Zhou, Z. Zhu, H. J. Park, C. Kwak, *Angew. Chem. Int. Ed.* **2011**, 50, 1792–1797; *Angew. Chem.* **2011**, 123, 1832–1837.
- [10] S. B. Adler, *Chem. Rev.* **2004**, 104, 4791–4843.
- [11] Z. P. Shao, S. M. Haile, *Nature* **2004**, 431, 170–173.
- [12] D. M. Bastidas, S. Tao, J. T. S. Irvine, *J. Mater. Chem.* **2006**, 16, 1603–1605.
- [13] G. Kim, S. Wang, A. J. Jacobson, L. Reimus, P. Brodersen, C. A. Mims, *J. Mater. Chem.* **2007**, 17, 2500–2505.
- [14] J. H. Kim, A. Manthiram, *J. Electrochem. Soc.* **2008**, 155, B385–B390.
- [15] J. H. Kim, M. Cassidy, J. T. S. Irvine, J. Bae, *Chem. Mater.* **2010**, 22, 883–892.
- [16] S. Yoo, J. Shin, G. Kim, *J. Mater. Chem.* **2011**, 21, 439–443.
- [17] A. Jun, J. Kim, J. Shin, G. Kim, *Int. J. Hydrogen Energy* **2012**, 37, 18381–18388.
- [18] S. Yoo, S. Choi, J. Kim, J. Shin, G. Kim, *Electrochim. Acta* **2013**, 100, 44–50.
- [19] S. Choi, S. Yoo, J. Kim, S. Park, A. Jun, S. Seongodan, J. Kim, J. Shin, H. Y. Jeong, H. Y. Y. Choi, G. Kim, M. Liu, *Sci. Rep.* **2013**, 3, 2426–2431.
- [20] A. Tarancón, J. Peña-Martínez, D. Marrero-López, A. Morata, J. C. Ruiz-Morales, P. Nuñez, *Solid State Ionics* **2008**, 179, 2372–2378.
- [21] W. Lee, J. W. Han, Y. Chen, Z. Cai, B. Yildiz, *J. Am. Chem. Soc.* **2013**, 135, 7909–7925.
- [22] Y. Shen, H. Zhao, X. Liu, N. Xu, *Phys. Chem. Chem. Phys.* **2010**, 12, 15124–15131.
- [23] S. B. Adler, X. Y. Chen, J. R. Wilson, *J. Catal.* **2007**, 245, 91–109.
- [24] M. Burriel, J. Peña-Martínez, R. J. Chater, S. Fearn, A. V. Berenov, S. J. Skinner, J. A. Kilner, *Chem. Mater.* **2012**, 24, 613–621.
- [25] A. Tarancón, S. J. Skinner, R. J. Chater, F. Hernández-Ramírez, J. A. Kilner, *J. Mater. Chem.* **2007**, 17, 3175–3181.
- [26] S. Yoo, S. Choi, J. Shin, M. Liu, G. Kim, *RSC Adv.* **2012**, 2, 4648–4655.
- [27] S. Yoo, S. Choi, J. Shin, G. Kim, *J. Electrochem. Soc.* **2011**, 158, B632–B638.